energies

MDPI

Article

Modelling and Simulating Eulerian Venturi Effect of SBM to Increase the Rate of Penetration with Roller Cone Drilling Bit

Dennis Delali Kwesi Wayo [1], Sonny Irawan [1,*], Alfrendo Satyanaga [2,*] and Ghulam Abbas [3]

[1] Department of Petroleum Engineering, School of Mining and Geosciences, Nazarbayev University, Astana 010000, Kazakhstan; dennis.wayo@nu.edu.kz
[2] Department of Civil and Environmental Engineering, School of Engineering and Digital Sciences, Nazarbayev University, Astana 010000, Kazakhstan
[3] Department of Petroleum and Natural Gas Engineering, Mehran University of Engineering and Technology, Shaheed Zulfiqar Ali Bhutto Campus, Khairpur Mir's 66020, Pakistan; engr_abbas@muetkhp.edu.pk
* Correspondence: irawan.sonny@nu.edu.kz (S.I.); alfrendo.satyanaga@nu.edu.kz (A.S.); Tel.: +7-7172705800 (S.I.); +7-7714912838 (A.S.)

Abstract: Drilling bits are essential downhole hardware that facilitates drilling operations in high-pressure, high-temperature regions and in most carbonate reservoirs in the world. While the drilling process can be optimized, drilling operators and engineers become curious about how drill bits react during rock breaking and penetration. Since it is experimentally expensive to determine, the goal of the study is to maximize the rate of penetration by modeling fluid interactions around the roller cone drilling bit (RCDB), specifying a suitable number of jet nozzles and venturi effects for non-Newtonian fluids (synthetic-based muds), and examining the effects of mud particles and drill cuttings. Ansys Fluent k-epsilon turbulence viscous model, a second order upwind for momentum, turbulent kinetic energy, and dissipation rate, were used to model the specified 1000 kg/m^3 non-Newtonian fluid around the roller cone drill bit. The original geometry of the nozzles was adapted from a Chinese manufacturer whose tricone had three jet nozzles. The results of our six redesigned jet nozzles (3 outer, 39.12 mm, and 3 proximal, 20 mm) sought to offer maximum potential for drilling optimization. However, at a pressure of 9.39 × 10^4 Pa, the wellbore with particle sizes between 0.10 mm and 4.2 mm drill cuttings observed an improved rate of penetration with a rotation speed of 150 r/min.

Keywords: synthetic-based mud; drill bits; Ansys Fluent; k-epsilon turbulence; ROP

check for updates

Citation: Wayo, D.D.K.; Irawan, S.; Satyanaga, A.; Abbas, G. Modelling and Simulating Eulerian Venturi Effect of SBM to Increase the Rate of Penetration with Roller Cone Drilling Bit. *Energies* **2023**, *16*, 4185. https://doi.org/10.3390/en16104185

Academic Editors: Krzysztof Skrzypkowski and Hossein Hamidi

Received: 7 February 2023
Revised: 1 May 2023
Accepted: 4 May 2023
Published: 18 May 2023

1. Introduction

Fluid (mud) design is crucial for downhole tools in the petroleum industry. The rheological profiles [1] of these engineered fluids must be suitable for cooling and lubricating drilling bits in the HPHT reservoirs.

Drill bits [2] are said to have the highest potency for crushing formation rocks and creating holes subsurface. The roller cone drill bit (RCDB) [3], which is being investigated in this study, crushes the floor of the formation bed with exerted weights from the drill bit, rotation of the drill pipe, and the jet impact force of fluids from the drill bit nozzles. Noticeably, there is a considerable amount of heat generated from RCDB cutters during rock interactions in the formation [4,5]. The continuous thermal cooling and friction effect add an economic cost to the design and replacement of drill bits; for this reason, engineering synthetic-based muds (SBM) for this study as proposed by Van Ort [6] helps to prevent accelerated wear of the drilling bit and effectively transports solid formation particles to the surface.

Nozzles of drill bits, non-Newtonian fluids (SBM), and the lithology of the formation [7] predict ROP optimization for this study. A constant rotation speed set at about 150 r/min for soft shale and other formation drill cuttings is shown in Figure 1, and the properly designed fluid hydraulics can be used to prevent the accumulation of drill cuttings on the surfaces of the drilling bits (balling) and also reduce the power consumption. Due to the difficulty of accurately reproducing well conditions [8], experimental methods to create bit design are costly. Real-time data evaluation should go hand in hand with the choice and optimization of the drill bit and drilling parameters if you want to obtain the best drilling performance at the lowest possible cost and time. The fluid flow pattern should be tuned for the pressure distribution and velocity profile beneath the drill bit in order to support the improvement in drilling hydraulics.

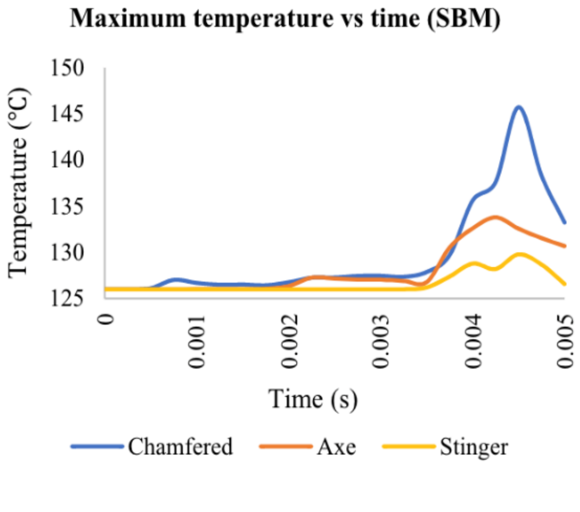

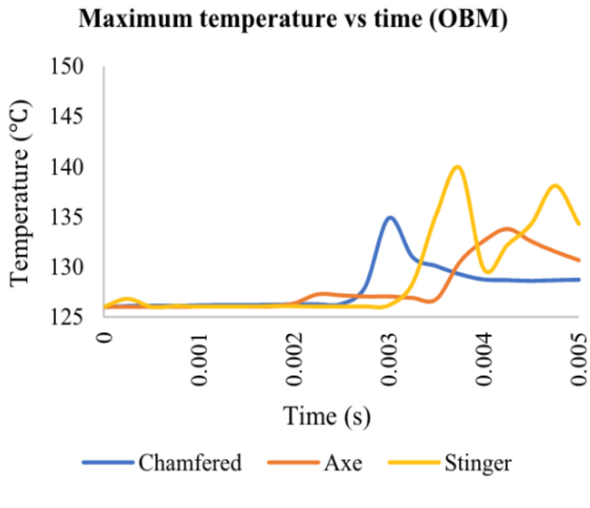

Figure 1. Compatibility of redesigned geometric cutters with fluid hydraulics (**a**) Chamfered cutter for SBM and (**b**) Stinger cutter for OBM adapted from [5] [Copyright license number 1294955-1].

The impact of bit design elements might be comprehended and used to enhance bit hydraulics with the aid of computational methodologies. A computational technique [9–13] called computational fluid dynamics (CFD) is useful for modeling fluid flow phenomena in drill bit designs with complex geometries that involve bit rotation and multi-phase conditions downhole of the well. Through the application of CFD to improve drill bit design, drilling performance can be boosted.

Moslemi and Ahmadi (MA) [14] used one of the computational methods to track spherical particles from the bottom of the wellbore to the surface. Their discrete particle modeling sought to compare the cutting-transport ratio (C_t) with the rate of penetration using a polycrystalline diamond compact (PDC) drill bit. Simulation results explain that hydraulic performance is further achieved if the nozzle jet velocity increases and the cutting-transport ratio (C_t) increases too. Interestingly, MA's model elaborates that the C_t at certain instances decreased slightly with seven nozzles as compared to a five-nozzle PDC drill bit. Further, a finite element modelling to investigate the thermal-mechanical wear of (PDC) drill bit in the wellbore and its influence on rate of penetration (ROP) was conducted by earlier researchers [5]. Their redesign of drill bit hydraulics and cutters resulted that chamfered geometric cutter was better with synthetic-based muds (SBM) while stinger designed cutter was also better with oil-based muds (OBM) as demonstrated in Figure 1. However, to define the robustness of cutters under different fluid rheological effect expounded that the periods between 0.004 to 0.005 s appears that the chamfered cutters in Figure 1a was able to withstand extreme temperature at 145 °C under the influence of SBM rheology. Similarly, Stinger at same periods was able to withstand 140 degrees Celsius based on OBM in Figure 1b.

Interestingly, the cost-time index of drill operations is meant for drill managers and operators to determine and devise magnificent means of optimizing cost and time to achieve better returns on investment without disconcerting environmental and safety standards in the oil and gas industry. However, optimizing the rate of penetration (ROP) [15,16] in drilling wells is one of the logical ways to determine whether or not the efficiency of drilling is achieved. The relationship between ROP and drilling cost is inversely proportional; a higher ROP reduces the cost of drilling operations [17].

Excerpts from researchers demonstrate the need to optimize drilling operations in the petroleum industry [18]. The challenge of simulating pressure-velocity profiles of synthetic-based muds around roller cone drill bits is because of the substantial design parameters and the applicable physics for simulations. While focusing on Eulerian–Eulerian flow equations [19], the study used Ansys Fluent for its 3D simulation analysis and was set to:

- Redesign tricone or RCDB considering Hebei Crossing Drill Bit.
- Resize, design, and increase the number of RCDB nozzles.
- Define flow restrictions in the wellbore and in the drill bit.
- Optimize ROP by investigating the flow of muds and particle sizes in single phase.

2. Methods

This part of the section exposes the novelty of the current research by considering the structural framework of the models used to comprehend the impact and the significance of synthetic-based mud (SBM) [20] on the rate of penetration, and elaborating a predictive analysis for the venturi effect of the drilling fluids in drill bits.

2.1. Drilling Data

The conventional means of drawing analysis is through acceptable structured data. The very objectives of this current study employed data from an open source, which come from an oilfield. For the above listed objectives, the 4-year data are filtered to give applicable meaning to the current research. However, it examines the depth (m), weight on bit (kg/m), speed of rotation (m/s), jet impact force (kg), and rate of penetration (m/h), as illustrated in Table 1 from its original imperial units.

Table 1. A 4-year sampled oilfield drilling data [21].

Imperial Units										
Depth, ft	3231	3592	3608	4021	4156	4156	4251	4267	4500	4749
WOB (klb/in)	1.57	2.86	3.29	1.86	4.00	3.14	2.57	3.00	2.86	2.57
Rotary Speed (r/min)	155	160	165	165	190	155	160	180	165	155
Jet impact force (klb)	1.86	1.82	2.35	1.77	1.85	2.16	2.00	1.96	2.22	2.24
ROP (ft/h)	31.3	25.3	45.0	16.5	32.2	35.6	15.9	29.5	22.0	17.6
Metric Units										
Depth, m	984.81	1094.8	1099.7	1225.60	1266.74	1266.74	1295.70	1300.58	1371.60	1447.49
WOB (kg/m)	28,062	51,120	58,805	33,245	71,496	56,124	45,936	53,622	51,120	45,936
Rotary Speed (m/s)	0.93	0.96	0.99	0.99	1.13	0.93	0.99	1.07	0.99	0.93
Jet impact force (kg)	843.68	825.54	1065.94	802.86	839.15	979.80	907.18	889.04	1006.98	1016.05
ROP (m/h)	9.54	7.71	13.72	5.03	9.81	10.85	4.85	8.99	6.71	5.36

As labeled in Table 1, several factors contribute to the optimization of the rate of penetration. The factors listed in Tables 1 and 2 cannot be justified without drilling fluids. The current research takes solace in the earlier scientific research conducted by Okon et. al. [22] whose synthetic-based drilling fluid was considered the main contributor in this current research. Drilling fluids coupled with the exerting weight on the drill bit generate enough force to keep crushing the formation bed in the wellbore. Cuttings [23] from the said formation are expected to interact with the drilling fluids to loosen up and fill up the void spaces [24]. Figure 2 illustrates expected cuttings from different formations.

Table 2. IADC Recommended drilling parameters for drill bit application [25].

Type/IADC code	116, 117	126, 127	136, 137	216, 217	317	337
WOB (kN/mm)	0.35~0.9	0.35~1.00	0.35~1.05	0.35~1.20	0.70~1.30	0.80~1.40
RPM (r/min)	150~80	150~70	120~60	90~50	80~45	75~45

Figure 2. Some expected drill cuttings adapted from [13] [Copyright License number 1337919-1].

2.2. Ansys Framework

An effective drilling optimization is better achieved by the nature of the drilling cuttings from the formation that is being drilled, as illustrated in Figure 2. The rate of penetration (ROP) coupled with non-Newtonian fluids (SBM) is modeled and simulated using Ansys Fluent. The algorithm in Figure 3 explains how drilling fluids can be used to optimize ROP.

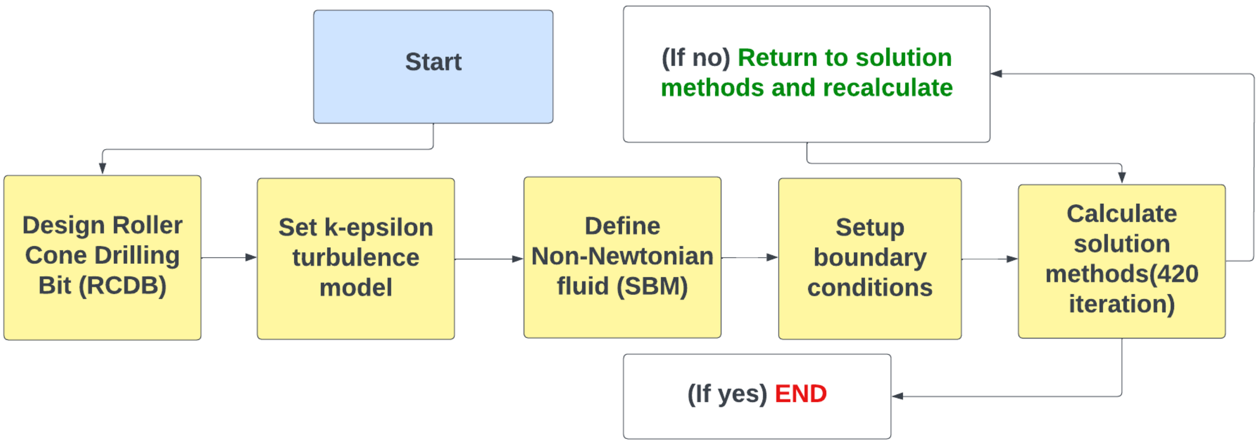

Figure 3. Ansys Fluent Algorithm for ROP optimization.

There are two main guides for validating ROP from the drilling data in Table 1. The field data are termed 'dirty data' because considerable data scrutiny must be conducted to suit the current study. The data are limited to the weight on the drilling bit, the jet force, and the drill pipe rotation.

The other aspect of validating the drilling process is to define the pressure-velocity of the non-Newtonian fluid; synthetic-based mud takes into account continuity and momentum. The cross-sectional structure of the roller cone drilling bit with an accurate metric design, as shown in Figure 4, reveals the inner venturi and exposes how fluids are expected to flow in three dimensions.

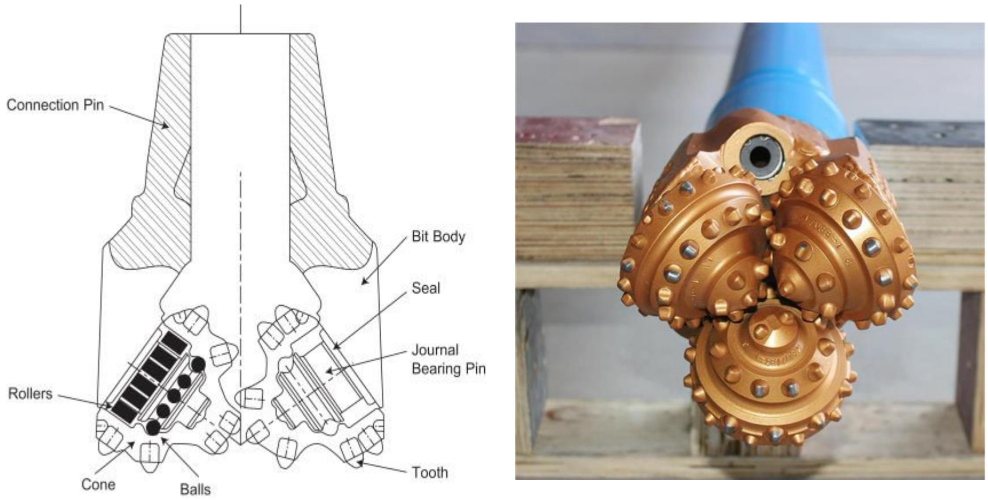

(**a**) (**b**)

Figure 4. Roller Cone Drill Bit (RCDB) (**a**) Cross-sectional view adapted from [3] [Copyright license number 5515440359124] (**b**) 3D view of Hebei's tricone with 3 nozzles [25].

The Reynolds number for the simulation process is expected to be high at different pressures and velocities; this was set to 4000. The k-epsilon turbulence model was set to define kinetic energy and dissipation rate in a 2nd order upwind.

2.3. Modelling

During ground breaking, particles ranging in size from 0.10 mm to 4.2 mm, based on vibratory sieving and image analysis, move in the drilling wells [26]. Most often, it is difficult to define the physics around particle dispersion in reference to drill cuttings and non-Newtonian fluid particles. Earlier studies conducted by [27] applied Eulerian equations to determine fluid particle-particle behavior in aid of removing filter cakes and transporting drill cuttings to the surface.

This section of the current study models ROP and demonstrates the venturi effect in the drilling bit.

2.3.1. ROP Model

There have been several proposed models for ROP and Table 3 selects a few traditional models relevant to this study. The importance of these models defines the tendency of bits coupled with drilling fluids to efficiently cut through the formation beds in the well.

Table 3. Modelling ROP.

Author	Equation	Models	Focus
Bourgoyne and Young [28]	(1)	$\frac{dD}{dt} = exp\left[\left(a_1 + \sum_{j=2}^{8} a_j x_j\right)\right]$	Widely used in the oil and gas industry.
Maurer [29]	(2)	$\mathrm{ROP} = \frac{\mathrm{K}}{\mathrm{S}^2}\left(\frac{\mathrm{W}}{\mathrm{d_b}} - \frac{\mathrm{W_o}}{\mathrm{d_b}}\right)^2 \mathrm{N}$	Rolling cutting bit.
Motahhari et al. [2]	(3)	$\mathrm{ROP} = \mathrm{W_f}\frac{\mathrm{GN^{y}N^{\alpha}}}{\mathrm{d_b S}}$	Polycrystalline diamond compact (PDC) bit.

Undoubtedly, Bourgoyne and Young's ROP model is widely used in the oil and gas industry today [30]. The development of this model in 1974 considered eight different parameters where a_1 to a_8 denote the strength of the drilled formation, drill bit tooth, pore pressure, pressure difference, weight on the drill bit, hydraulic jet impact, formation compaction, and rotary drilling. However, t and D denotes time and depth, respectively.

Maurer [29] developed Equation (2) in Table 3; its model places emphasis on rolling cutting bits, which is paramount to this study since the current study simulates roller cone drilling bits. Maurer, in this Equation (2), explains how rock debris or cuttings are removed from the teeth of the drilling bit to optimize perfect cleaning. W and W_o represent weight on the bit and weight on the bit threshold, where K denotes the drillability constant, N and d_b also denote rotary speed and drill bit diameter, respectively.

The modeling of a polycrystalline diamond compact bit proposed by Motahhari et al. considers w_f as wear, G as bit geometry, rock interaction coefficient α and y are ROP coefficients, and S represents rock strength [31].

2.3.2. General Equations

The continuity equation is used to express the volume percentage of the solid-liquid flow in the hypothetical wellbore. The force, mass, and speed of the solid-fluid movement in the wellbore are described by the sum of all momentum acting on the solid-liquid phases; and Equations (4) and (5) are models considered from Epelle-Gerogiorgis (EG) [27].

Volume fraction solid phase a_s, solid phase density ρ_s, liquid phase density ρ_l, liquid velocity $\vec{v}_s$, velocity interphases $\vec{v}_{ls-sl}$, gravity (g), mass transfers $\dot{m}_{ls-sl}$, and external force $\vec{F}_s$ are all included in the flow continuity and momentum parameters. The high-pressure injection of drilling fluids and the rotational speed of the drilling pipe in the wellbore, however, make Equation (2)'s turbidity force relevant.

Momentum,

$$\frac{1}{\rho_{rs}}\left(\frac{\partial}{\partial t}(a_s\rho_s)+\nabla\cdot\left(a_s\rho_s\vec{v}_s\right)=\sum_{l=1}^{n}(\dot{m}_{ls}-\dot{m}_{sl})\right), \tag{4}$$

$$\frac{\partial}{\partial t}\left(a_s\rho_s\vec{v}_s\right)+\nabla\cdot\left(a_s\rho_s\vec{v}_s\vec{v}_s\right)$$

$$=-a_s\nabla p-\nabla p_s \quad +\nabla\cdot\bar{\bar{\tau}}_q+a_s\rho_s\vec{g} + \sum_{l=1}^{n}\left(K_{ls}\left(\vec{v}_l-\vec{v}_s\right)+\dot{m}_{ls}\vec{v}_{ls}-\dot{m}_{sl}\vec{v}_{sl}\right)+\begin{pmatrix}\vec{F}_s+\vec{F}_{lift,s}\\+\vec{F}_{vm,s}+\vec{F}_{td,s}\end{pmatrix},$$

$$\frac{\partial}{\partial t}\left(a_s\rho_s\vec{v}_s\right)+\nabla\cdot\left(a_s\rho_s\vec{v}_s\vec{v}_s\right)$$

$$=-a_s\nabla p-\nabla p_s+\nabla\cdot\bar{\bar{\tau}}_q+a_s\rho_s\vec{g}+\sum_{l=1}^{n}\left(K_{ls}\left(\vec{v}_l-\vec{v}_s\right)\right)+\begin{pmatrix}\vec{F}_s+\vec{F}_{lift,s}\\+\vec{F}_{vm,s}\end{pmatrix}. \tag{5}$$

Previous research [19,27,32] has provided explanations for the effective review of the solid-liquid exchange coefficient, K_{sl}. When the volume percentage of the liquid phase, $a_l > 0.8$, then, K_{sl}, is transformed from Equations (6)–(9). The current study does not, however, predict that the fluid will flow in a uniform laminar flow due to the rotating drill pipe and the release of drilling fluids [33] from the bit's nozzles to improve rate of penetration. Under these conditions, a turbulence model would be created by the pressure and velocity scales, and high Reynolds numbers would be anticipated. For this model, it was thought that the variables changing around the transport equation in a single-phase flow represented by Equations (10) and (11) would affect the rate of dissipation (k) and the kinetic energy (ε).

Solid-liquid exchange coefficient,

$$K_{sl} = \frac{3}{4} C_D \frac{\left(a_s a_l \rho_l \left| \vec{v}_s - \vec{v}_l \right| \right)}{d_s} {a_l}^{-2.65}, \tag{6}$$

Drag coefficient;

$$C_D = \frac{24}{a_l Re_s} \left[1 + 0.5 (a_l Re_s)^{0.687}\right], \tag{7}$$

Reynolds number of the solid particle phase;

$$Re_s = \frac{\left(\rho_l d_s \left| \vec{v}_s - \vec{v}_l \right| \right)}{\mu_l}, \tag{8}$$

where $a_l \leq 0.8$, then,

$$K_{sl} = 150 \frac{a_s (1 - a_l) \mu_l}{a_l {d_s}^2} + 1.75 \frac{\rho_l a_s | \vec{v}_s - \vec{v}_l |}{d_s}. \tag{9}$$

Dissipation rate and Kinetic energy,

$$\frac{\partial}{\partial t} (C_\alpha \rho_\alpha k_\alpha) + \nabla \cdot \left(C_\alpha \left(\rho_\alpha U_\alpha k_\alpha - \left(\mu + \frac{\mu_{t\alpha}}{\sigma_k} \right) \nabla k_\alpha \right) \right) = C_\alpha (P_\alpha - \rho_\alpha \varepsilon_\alpha) + T_{\alpha\beta}^{(k)} \tag{10}$$

$$\frac{\partial}{\partial t} (C_\alpha \rho_\alpha \varepsilon_\alpha) + \nabla \cdot \left(C_\alpha \rho_\alpha U_\alpha \varepsilon_\alpha - \left(\mu + \frac{\mu_{t\alpha}}{\sigma_\varepsilon} \right) \nabla \varepsilon_\alpha \right) = C_\alpha \frac{\varepsilon_\alpha}{k_\alpha} (C_{\varepsilon 1} P_\alpha - C_{\varepsilon 2} \rho_\alpha \varepsilon_\alpha) + T_{\alpha\beta}^{(\varepsilon)}. \tag{11}$$

2.4. CFD Simulations

Simulating ROP at the wellsite is a cost-effective aspect to consider. Experimental techniques can be very expensive, both in the field and in the laboratory. Substantive data from the fields can be readily modeled and simulated to achieve the target goals, optimizing drilling conditions. The pressure-velocity profiles were monitored using the data in Tables 1 and 2 with Ansys Fluent software. Fluid turbulence around the complex mill teeth of roller cone drill bits (RCDB) was simulated to optimize the rate of penetration.

The mill-teeth CJ117 TCI tricone bit from the Chinese manufacturer Hebei Crossing Drill Bit [25], with a size of 17.5 inches, is used in this investigation. Moreover, with three jet nozzles and an inner diameter of 39.12 mm, the product is capable of drilling both oil and water wells. The mill-teeth CJ117 TCI tricone entire drill bit weight is 250 kg.

2.4.1. Assumptions

The efficacy of simulating ROP optimization with the said non-Newtonian fluid (synthetic-based mud) considers the following assumptions:

- The diameter of the well is the size of the drill bit at 444.5 mm.
- The diameter of each jet nozzle is set to 39.12 mm.
- The length of the drill bit is assumed to be 380 mm.
- The study holds the efficiency of the non-Newtonian fluid constant, since this has already been proven in our earlier research.
- The flow of fluid is in a single phase and no particles or drill cuttings collisions are expected.
- Heat is assumed to have been generated at 66.85 °C (340 °K) [34].
- The speed of drill bit rotation was assumed at 150 r/min.
- The mill tooth of the 250 kg drill bit is excluded to ease the complexity of the simulation.

2.4.2. Geometry, Boundary, and Mesh

Modeling fluid behavior in drill bits and its interactions with other drill cuttings (solid formation particles) in the wells to optimize the rate of penetration is a complex situation. The applied geometry considers the above simulation assumptions to reduce the extended difficulties in real time.

DesignModeler from Ansys 2022 R2 was used to design a 444.5 mm geometry roller cone drilling bit. The three nozzles of the drill bit in modern design were considered, and Figure 5 shows an additional three nozzles at the center of the drill bit that were created to support the purpose of the current study by optimizing the rate of penetration.

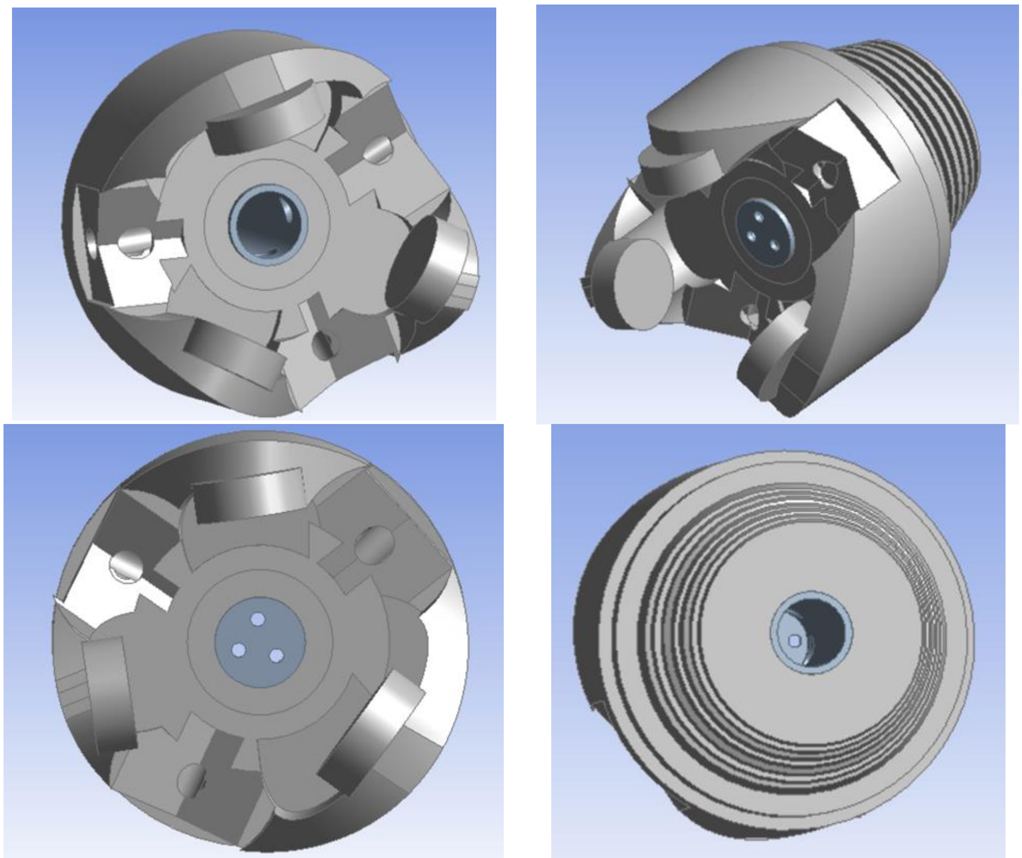

Figure 5. 3D RCDB Geometry.

Successful geometry was imported into the mesh setup, and CFD Fluent was selected for the applicable simulation. The boundaries of the designed drill bit were selected at a maximum thickness of 2 mm and 1.5 mm at two different inflation options, as depicted in Figure 6. Moreso, during meshing, the element and maximum size of the drill bit were set to 1.22 mm and 2.44 mm, respectively, and the tetrahedral mesh generated a total number of nodes of 240,813 and elements of 660,087 in Figure 7.

Figure 8a,b complete the complexity of the simulation conducted. The inner walls of the roller cone drill bit were extracted from the main design. The vertical cylinder and curved pipes represent the flow of the synthetic-based mud or non-Newtonian fluids through the inlet to the nozzles and from the 6 nozzles to the formation bed.

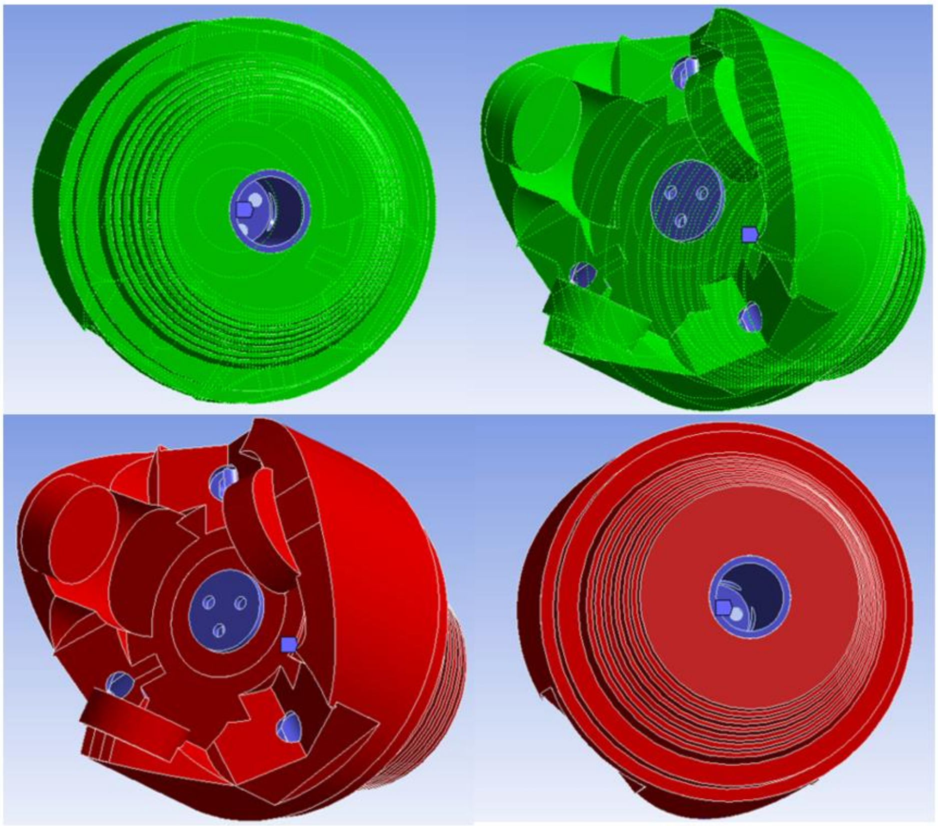

Figure 6. 3D RCDB Boundaries.

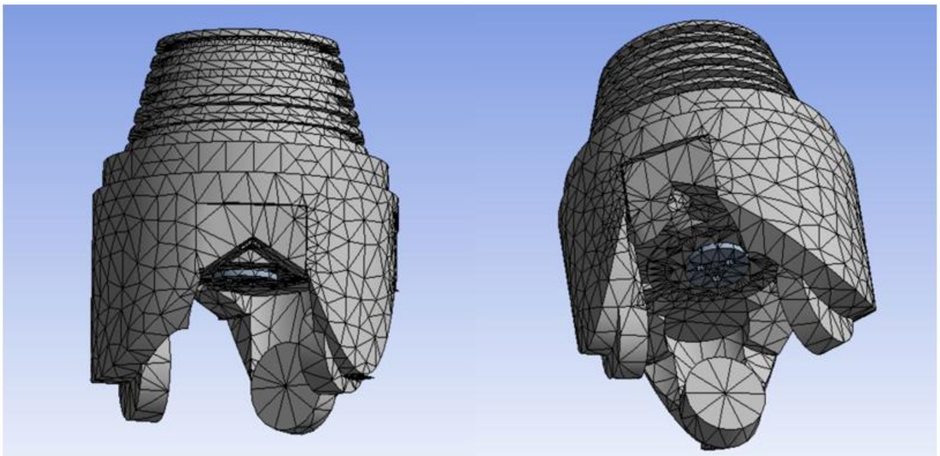

Figure 7. 3D RCDB Mesh.

However, the same design processes were conducted for the mud flow, from the geometry through boundaries, mesh, and final simulation. While simulating, the energy equation for the model was turned on, and the turbulent kinetic energy and its dissipation for the liquid-solid (SBM) were set to a 2nd order upwind. The density of the mud was 1000 kg/m^3, with an inlet velocity of 2 m/s and a temperature of 66.85 °C (340 °K). The simulation process was set to iterate 420 times but was conducted at 125, and this reveals faster computational analysis, aiding better decision-making prognosis.

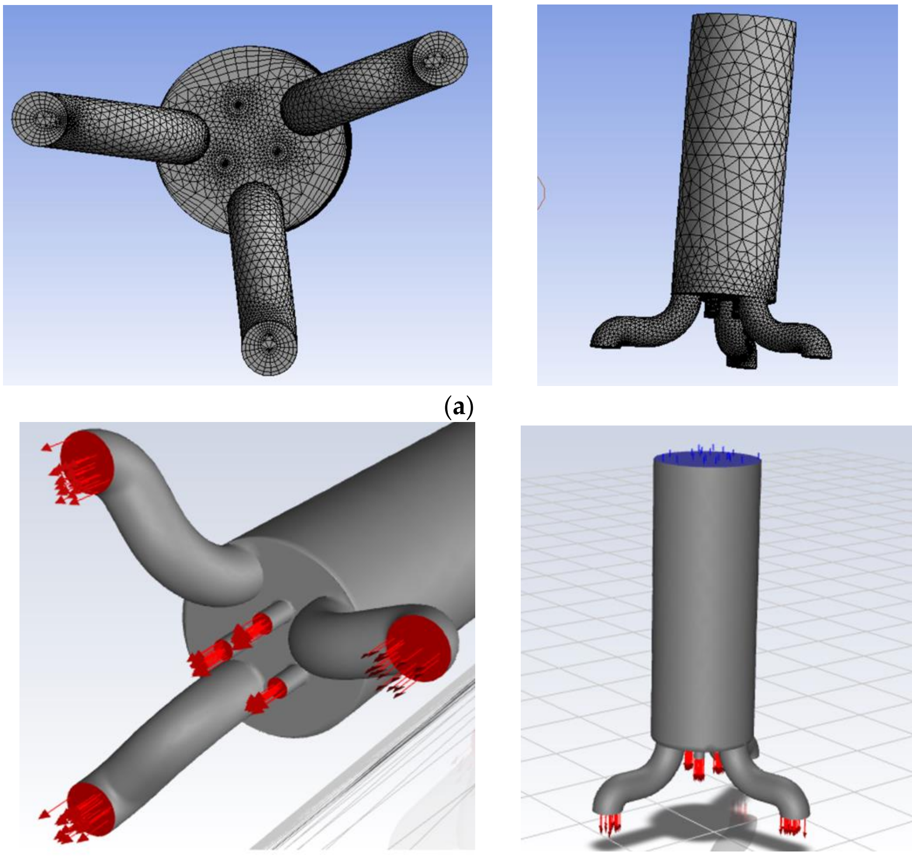

(**a**)

(**b**)

Figure 8. Extraction of fluid container from the 3D RCDB (**a**) mesh (**b**) mesh shows flow directions.

3. Results and Discussion

Several unanticipated factors arise when the wellbore penetration rate is optimized. The pressure and velocity profiles for the simulated roller cone drill bit are discussed in this section.

Drill bit nozzles are crucial in maximizing the rate of penetration. To increase the drilling bit's effectiveness in the wellbore, research on the design of the original three nozzles led to the creation of three more nozzles. The newly created nozzles have a diameter of 20 mm, as opposed to the three original nozzles' 39.12 mm sizes. Figure 8's nozzles show higher jet velocities, with each nozzle displaying an inlet velocity of 10 m/s. In this investigation, the empirical finding that the 39.12 mm diameter nozzle outflows slower at a reduced pressure than the 20 mm diameter nozzles do not need to be questioned. However, the geometry of the aforementioned design caused the flow to become turbulent by increasing the Reynolds number to over 4000. Based on the venturi effect emanating from the structural design of the roller cone drill bit, this gives rise to the absence of laminar flow. Modern modeling of nozzles in drill bits raises an objective means to consider when optimizing penetration in the wellbore. Not far from the intended research guide [35,36], we propose that an additional three 13 mm nozzles can bring the safe drilling operation optimization we seek.

Solid particles emanating from the synthetic-based mud or the non-Newtonian fluids coupled with the cuttings from the formation bed influenced the simulation process [37,38]. Figure 9 demonstrates the flow velocities of these muds at different nozzles, and the interaction with the drill cuttings had an adverse effect on the rate of penetration optimization. Nonetheless, an increase in the drill cuttings and mud particles in the simulation reduces the rotation speed of the drill bit and hence affects the net ROP. Conversely, what the simulation study sought to have achieved was the ROP optimization, hence, an RPM of

150 r/min, as stipulated in Table 2, achieved a greater result by overcoming the weights of the said particles both in the mud and cuttings for perfect hole cleaning [39].

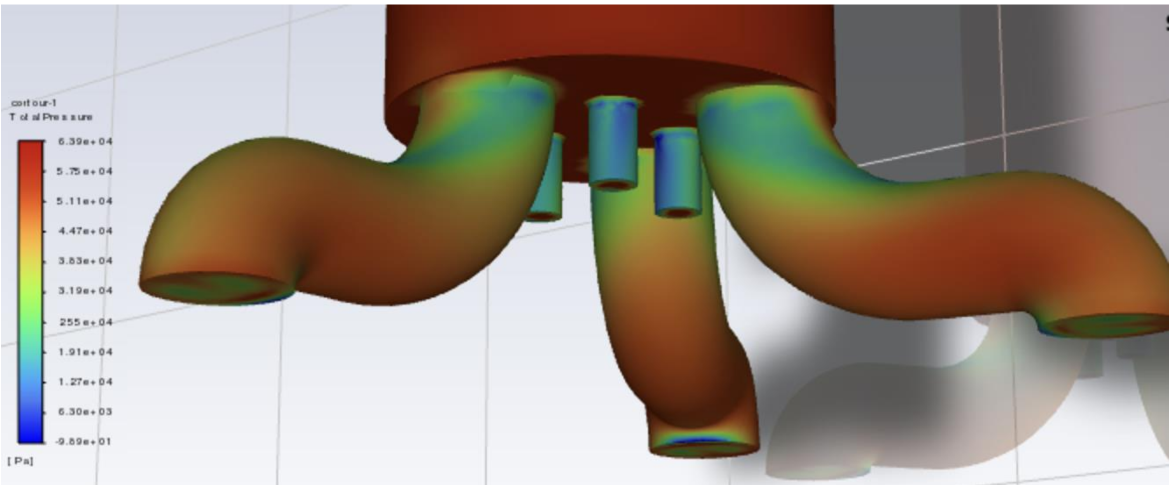

Figure 9. 3D RCDB nozzles simulated velocity-pressure profile.

Our Ansys Fluent-based 3D simulation study was compared to Kirencigil and Sivagnanam's (KS) [40,41] simulation model, which took the polycrystalline diamond compact (PDC) drill bit into account. The comparison of the design parameter summary, which includes the simulation's geometry and flow rates, is provided in Table 4. Though six standard round nozzles were considered based on KS and Ansys Fluent models, Wells et al. [42] in Houston investigated and presented various nozzle geometries for ROP optimization with an emphasis on roller cone and PDC drill bits. Their analyses were also compared to the current study based on pressure-velocity-turbulence profiles. As indicated in Figure 10, the shape, inlet, and outlet of the nozzles (standard circular, star, slot, Y, cross, flute, dual-jet, and K) did not significantly modify the jet flow compared to the round nozzles based on an equal optimization numerical analysis. This, however, validates the current study based on the conventional nozzle used for roller cone bit ROP optimization investigations.

Table 4. Ansys Fluent fluid-drill bit simulation parameters for validation.

	Drill Bit	Solver	Viscous Model	Fluid	Boundary	Solution Methods
Kirencigil [41]	Polycrystalline diamond compact	Pressure-based steady state	k-omega	Liquid-solid ρ = 949 kg/m^3 μ = 0.005 kg/m·s	Inlet velocity = 16 m/s Outflow (standard wall)	Simple pressure-velocity coupling, 1st order upwind for momentum, turbulent kinetic energy, dissipation rate
Sivagnanam [42]	Polycrystalline diamond compact	Pressure-based steady state	k-omega	Liquid-solid ρ = 1500kg/m^3 μ = 0.04kg/m·s	Inlet velocity = 57 m/s Outflow (standard wall)	Simple pressure-velocity coupling, 1st order upwind for momentum, turbulent kinetic energy, dissipation rate
Current Study	Tricone or roller cone drill bit	Pressure-based steady state	k-epsilon	Liquid-solid ρ = 1000 kg/m^3 μ = 0.06 kg/m·s	[Momentum (Inlet velocity at 20 m/s), Thermal at 340 °K] Outflow (standard wall)	Simple pressure-velocity coupling, 2nd order upwind for momentum, turbulent kinetic energy, dissipation rate

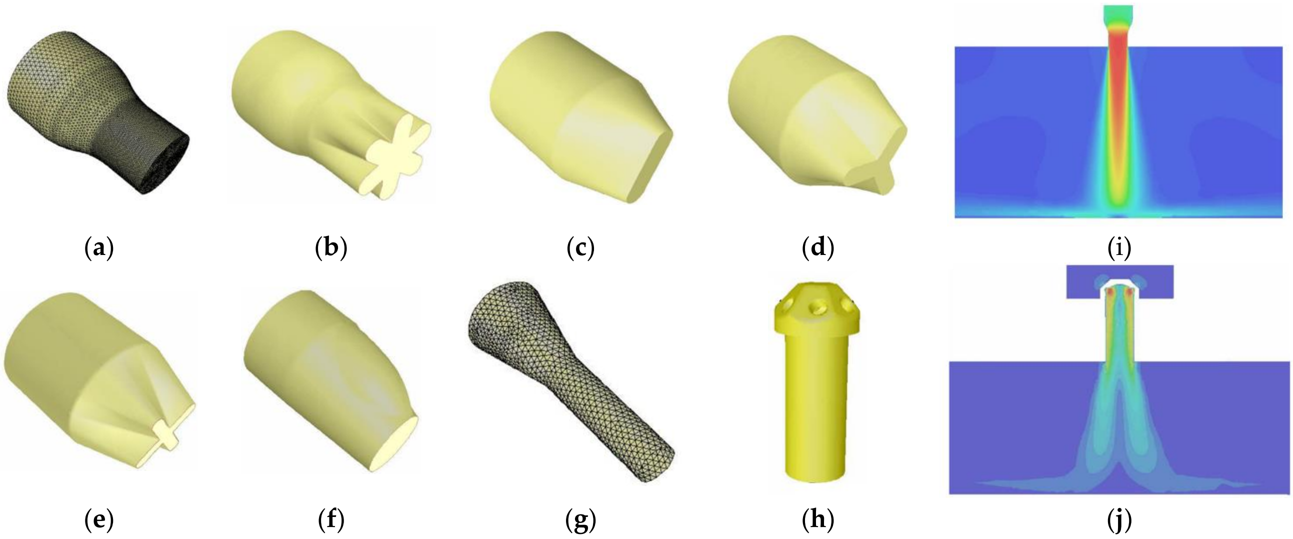

Figure 10. 3D nozzle geometry for jet flow-ROP investigation (**a**) standard circular nozzle, (**b**) star nozzle, (**c**) slot nozzle, (**d**) Y-nozzle, (**e**) cross nozzle, (**f**) flute nozzle, (**g**) dual-jet nozzle, (**h**) K-nozzle, (**i**,**j**) simulation of jet flow in standard circular nozzle (conventional) and K-nozzle (unconventional) adapted from Ref. [42], 2003, Wells, M.

Moreover, the parameters for the complex designs are not far from each other, as stipulated in Table 4. The current research uses a different viscous model, introduces a thermal condition to the flow, and increases the stability of the order upwind regarding momentum, turbulence, and dissipation rate. Moreover, the fluid type under examination selected the liquid-solid at a density of 1000 kg/m^3, as stipulated by the Ansys Fluent constants.

Nonetheless, the nozzle diameter for each simulation, as indicated by K-S models in Table 4, is considered pressure drops at 20 mm and 12 mm, respectively, whereas the current research focuses on the 39.12 mm and 20 mm nozzles. It is indicated that the pressure at the bottom of the drill bit is directly proportional to the size of the nozzles. The higher the pressure, the smaller the nozzles, and the lower the pressure, the bigger the nozzles.

KS model employed 6 and 7 nozzles for PDC drill bits, respectively; our current research employs 6 nozzles for roller cone drilling bit. While each of these authors explained the virtue of increasing the number of nozzles on PDC drill bits to improve the rate of penetration in the wellbore, Figure 9 further illustrates the fluid-nozzle investigation's overall pressure. The fact that the pressure increases from -9.69×10^1 Pa to 6.39×10^4 Pa is interesting since it actually explains why the initial pressure must begin at zero. The blue (low pressure) and red (high pressure) demarcations show where mud flow occurs at different pressures. Additionally, it could be noticed that the three 20 mm proximal nozzles started flowing with low pressure before subsequently regaining some adequate pressure. In a similar fashion, the flow in the three outer 39.12 mm nozzles started off at low pressure before being tuned at higher pressures. The rate of penetration is efficiently improved by the direct relationship between the flow rate of the 1000 kg/m^3 mud (non-Newtonian) and the overall pressure in the newly developed nozzles. It is crucial to note that at a pressure of 6.39×10^4 Pa, particles with sizes ranging from 0.10 mm to 4.2 mm in the wellbore would conveniently be carried by the fluid gel's ability to suspend and transport the said particles. Nevertheless, adding the extra three proximal nozzles to the simulation increases the total pressure needed to optimize ROP.

4. Conclusions

Fluid dynamics in the wellbore breeds excess curiosity for study. The flow of non-Newtonian fluids or synthetic-based mud around the roller cone drill bit for the optimization of the rate of penetration called for its simulation. The focus of this study is to encourage a redesign of flow paths that can contribute to the original flow geometry for ROP and drilling optimization.

- The 20 mm and 39.12 mm diameters of the six nozzles at an RPM of 150 r/min provided the required flow pressure-velocity profiling to improve ROP.
- The density and particle sizes of the mud and the drill cuttings observed an optimized rate of penetration at an RPM of 150 r/min.

The formulated synthetic-based mud used for this study can be again considered using nanoparticles for its mud designs to reduce the size of particle flow occupancy and movement in the near future. Additionally, the complexity of the drill bit design can be improved to further buttress nozzle simulations. Most importantly, the simulated drill bit is suitable and recommended for soft and low-compressive-strength rock formations, as shown in Figure 2. Most importantly, this current study admonishes fluid engineers in the oil and gas industries about the potential parameters to implement while simulating hydraulic fluids with redesigned drill bit concepts to obtain the ideal rate of penetration in extremely tight reservoirs. Prior to beginning drilling operations, this should let staff and management make an informed decision based on an accurate computer forecast.

Author Contributions: D.D.K.W. and S.I. designed the numerical simulation. D.D.K.W. computed the CFD workflow and wrote the manuscript. The methods and results of the manuscripts were reviewed by S.I., A.S. and G.A. Project administration and funding acquisition was performed by A.S. and S.I. All authors have read and agreed to the published version of the manuscript.

Funding: This research was funded by [Nazarbayev University] grant number [11022021CRP1512] And the APC was funded by [Nazarbayev University]. The authors are grateful for this support. Any opinions, findings, and conclusions or recommendations expressed in this material are those of the author(s) and do not necessarily reflect the views of Nazarbayev University.

Data Availability Statement: Data would be made available on request.

Acknowledgments: We are grateful to Nazarbayev University for providing us with the opportunity to continue sharing our work as part of the Collaborative Research Program (CRP) for the periods of 2022–2024 with project number 11022021CRP1512. We again show appreciation to the support of Faculty-Development Competitive Research Grant for 2020–2022 (batch 2) with project number 08042FD1911. We are also gratefully indebted to Jong Kim for his advice and coaching.

Conflicts of Interest: The authors hereby declare that the research presented in this paper was not impacted by any known conflicting financial interests or personal connections.

Nomenclature

CFD	computational fluid dynamic
RPM (r/min)	revolution per minute
OBM	oil-based mud
SBM	synthetic-based mud
a	ROP coefficient
a_n	formation and drill parameters
a_s	solid phase volume fraction
a_l	liquid phase volume fraction
C_D	drag coefficient
D	depth, m
d_b	drill bit diameter
d_s	particle diameter, m
E	distance between centers, m
e	eccentricity
ε_α	kinetic energy
$\vec{F}_s$	solid phase force, N
$\vec{F}_{lift,s}$	lift force, N

$\vec{F}_{vm,s}$	virtual mass force, N
$\vec{F}_{td,s}$	turbulence dispersion force, N
G	coefficient of bit-rock geometry
g	gravity, m/s^2
K	drillability constant
k_α	rate of dissipation
K_{ls}	interphase momentum exchange coefficient
$\dot{m}_{ls}$	mass transfer from liquid phase to solid phase, kg/s
$\dot{m}_{sl}$	mass transfer from solid phase to liquid phase, kg/s
NP_α	rotary speedvolume fraction pressure
P_s	solids pressure, Pa
ρ_s	solid phase density, kg/m^3
ρ_l	liquid phase density, kg/m^3
R_i	center of inner tube
Re_s	particle Reynolds number
R_o	center of outer tube, m
R_T	cuttings transport ratio
S	rock strength
t	time, hr
μ	viscosity, Pa·s
μ_l	fluid viscosity, Pa·s
$\mu_{t\alpha}$	turbulence viscosity, Pa·s
V_a	velocity of cuttings transport, m/s
V_t	fluid velocity in annulus m/s
$\vec{v}_l$	liquid phase velocity m/s
w_f	wear
w	weight on bit
w$_o$	weight on bit threshold
$\vec{v}_s$	solid phase velocity m/s

References

1. Sharma, P.; Kudapa, V.K. Rheological study of fluid flow model through computational flow dynamics analysis and its implications in mud hydraulics. *Mater. Today Proc.* **2021**, *47*, 5326–5333. [CrossRef]
2. Motahhari, H.R.; Hareland, G.; James, J.A. Improved Drilling Efficiency Technique Using Integrated PDM and PDC Bit Parameters. *J. Can. Pet. Technol.* **2010**, *49*, 45–52. [CrossRef]
3. Guo, B.; Liu, G. Equipment in Mud Circulating Systems. In *Applied Drilling Circulation Systems*; Gulf Professional Publishing: Houston, TX, USA, 2011; pp. 3–18. [CrossRef]
4. Esfahanizadeh, L.; Dabir, B.; Goharpey, F. CFD modeling of the flow behavior around a PDC drill bit: Effects of nano-enhanced drilling fluids on cutting transport and cooling efficiency. *Eng. Appl. Comput. Fluid Mech.* **2022**, *16*, 977–994. [CrossRef]
5. Ayop, A.Z.; Bahruddin, A.Z.; Maulianda, B.; Prakasan, A.; Dovletov, S.; Atdayev, E.; Rani, A.M.A.; Elraies, K.A.; Ganat, T.A.-A.; Barati, R.; et al. Numerical modeling on drilling fluid and cutter design effect on drilling bit cutter thermal wear and breakdown. *J. Pet. Explor. Prod. Technol.* **2020**, *10*, 959–968. [CrossRef]
6. Van Oort, E.; Lee, J.; Friedheim, J.; Toups, B. New flat-rheology synthetic-based mud for improved deepwater drilling. In Proceedings of the SPE Annual Technical Conference and Exhibition, Houston, TX, USA, 26–29 September 2004; pp. 4579–4589. [CrossRef]
7. Zakharov, L.; Martyushev, D.; Ponomareva, I.N. Predicting dynamic formation pressure using artificial intelligence methods. *J. Min. Inst.* **2022**, *253*, 23–32. [CrossRef]
8. Al-Rubaii, M.M.; Elkatatny, S.; Gajbhiye, R.; Alafnan, S.; Glatz, G.; Al-Yami, A.; Haq, B. A New Rate of Penetration Model Improves Well Drilling Performance. In Proceedings of the SPE Symposium: Unconventionals in the Middle East-From Exploration to Development Optimisation, Manama, Bahrain, 23–24 March 2022.
9. Riazi, M.; Mehrjoo, H.; Nakhaei, R.; Jalalifar, H.; Shateri, M.; Riazi, M.; Ostadhassan, M.; Hemmati-Sarapardeh, A. Modelling rate of penetration in drilling operations using RBF, MLP, LSSVM, and DT models. *Sci. Rep.* **2022**, *12*, 1–24. [CrossRef]
10. Ameur-Zaimeche, O.; Kechiched, R.; Aouam, C.-E. Rate of penetration prediction in drilling wells from the Hassi Messaoud oil field (SE Algeria): Use of artificial intelligence techniques and environmental implications. In *Computers in Earth and Environmental Sciences Artificial Intelligence and Advanced Technologies in Hazards and Risk Management*; Elsevier Inc.: Amsterdam, The Netherlands, 2022. [CrossRef]
11. Bizhani, M.; Kuru, E. Towards drilling rate of penetration prediction: Bayesian neural networks for uncertainty quantification. *J. Pet. Sci. Eng.* **2022**, *219*, 111068. [CrossRef]

12. Hazbeh, O.; Aghdam, S.K.-Y.; Ghorbani, H.; Mohamadian, N.; Alvar, M.A.; Moghadasi, J. Comparison of accuracy and computational performance between the machine learning algorithms for rate of penetration in directional drilling well. *Pet. Res.* **2021**, *6*, 271–282. [CrossRef]
13. Gan, C.; Cao, W.-H.; Liu, K.-Z.; Wu, M. A novel dynamic model for the online prediction of rate of penetration and its industrial application to a drilling process. *J. Process. Control.* **2022**, *109*, 83–92. [CrossRef]
14. Moslemi, A.; Ahmadi, G. Study of the Hydraulic Performance of Drill Bits Using a Computational Particle-Tracking Method. *SPE Drill. Complet.* **2014**, *29*, 28–35. [CrossRef]
15. Hegde, C.; Millwater, H.; Pyrcz, M.; Daigle, H.; Gray, K. Rate of penetration (ROP) optimization in drilling with vibration control. *J. Nat. Gas Sci. Eng.* **2019**, *67*, 71–81. [CrossRef]
16. Faronov, M.V.; Polushin, I.G. Observer-based control of vertical penetration rate in rotary drilling systems. *J. Process. Control.* **2021**, *106*, 29–43. [CrossRef]
17. Mustafa, A.B.; Abbas, A.K.; Alsaba, M.; Alameen, M. Improving drilling performance through optimizing controllable drilling parameters. *J. Pet. Explor. Prod. Technol.* **2021**, *11*, 1223–1232. [CrossRef]
18. Ponomareva, I.N.; Galkin, V.I.; Martyushev, D.A. Operational method for determining bottom hole pressure in mechanized oil producing wells, based on the application of multivariate regression analysis. *Pet. Res.* **2021**, *6*, 351–360. [CrossRef]
19. Shynybayeva, A. Eulerian–Eulerian Modeling of Multiphase Flow in Horizontal Annuli: Current Limitations and Challenges. *Processes* **2020**, *8*, 1426. [CrossRef]
20. Martyushev, D.A.; Govindarajan, S.K. Development and study of a visco-elastic gel with controlled destruction times for killing oil wells. *J. King Saud Univ.-Eng. Sci.* **2022**, *34*, 408–415. [CrossRef]
21. Paiaman, A.M.; Al-askari, M.K.G.; Salmani, B.; Masihi, M.; Alanazi, B.D. Effect of Drilling Fluid Properties on Rate of Penetration. *Nafta* **2009**, *60*, 129–134. Available online: https://core.ac.uk/download/pdf/14418076.pdf (accessed on 10 November 2022).
22. Okon, A.N.; Agwu, O.E.; Udoh, F.D. Evaluation of the cuttings carrying capacity of a formulated synthetic-based drilling mud. In Proceedings of the Nigeria Annual International Conference & Exhibition (NAICE 2015), Victoria Island, Lagos, Nigeria, 4–6 August 2015. [CrossRef]
23. Khan, J.A.; Pao, W.K. Effect of Different Qualities of Foam on Fill Particle Transport in Horizontal Well Cleanup Operation Using Coiled Tubing. *Adv. Mater. Res.* **2014**, *903*, 39–44. [CrossRef]
24. Galkin, S.V.; Martyushev, D.A.; Osovetsky, B.M.; Kazymov, K.P.; Song, H. Evaluation of void space of complicated potentially oil-bearing carbonate formation using X-ray tomography and electron microscopy methods. *Energy Rep.* **2022**, *8*, 6245–6257. [CrossRef]
25. Available online: www.crossingbit.com (accessed on 5 December 2022).
26. Kern, J.G.C.; Montagna, G.P.; Borges, M.F. Techniques for Determining Size and Shape of Drill Cuttings. *Braz. J. Pet. Gas* **2022**, *16*, 65–77. [CrossRef]
27. Epelle, E.I.; Gerogiorgis, D.I. CFD modelling and simulation of drill cuttings transport efficiency in annular bends: Effect of particle sphericity. *J. Pet. Sci. Eng.* **2018**, *170*, 992–1004. [CrossRef]
28. Bourgoyne, A.J., Jr.; Young, F.S., Jr. A Multiple Regression Approach to Optimal Drilling and Abnormal Pressure Detection. *Soc. Pet. Eng. J.* **1974**, *14*, 371–384. [CrossRef]
29. Maurer, W. The "Perfect—Cleaning" Theory of Rotary Drilling. *J. Pet. Technol.* **1962**, *14*, 1270–1274. [CrossRef]
30. Sauki, A.; Khamaruddin, P.N.F.M.; Irawan, S.; Kinif, I.; Ridha, S.; Ali, S.A.; Ali, M.A. Development of a modified Bourgoyne and Young model for predicting drilling rate. *J. Pet. Sci. Eng.* **2021**, *205*, 108994. [CrossRef]
31. Liu, C.; Zhang, L.; Li, Y.; Liu, F.; Martyushev, D.A.; Yang, Y. Effects of microfractures on permeability in carbonate rocks based on digital core technology. *Adv. Geo-Energy Res.* **2022**, *6*, 86–90. [CrossRef]
32. Huque, M.M.; Butt, S.; Zendehboudi, S.; Imtiaz, S. Systematic sensitivity analysis of cuttings transport in drilling operation using computational fluid dynamics approach. *J. Nat. Gas Sci. Eng.* **2020**, *81*, 103386. [CrossRef]
33. Al-Kayiem, H.; Khan, J. CFD Simulation of Drag Reduction in Pipe Flow by Turbulence Energy Promoters. *ARPN J. Eng. Appl. Sci.* **2016**, *11*, 14219–14224.
34. Renpu, W. Production Casing and Cementing. In *Advanced Well Completion Engineering*; Elsevier: Amsterdam, The Netherlands, 2011; pp. 221–294. [CrossRef]
35. Rashidi, B.; Hareland, G.; Wu, Z. Performance, simulation and field application modeling of rollercone bits. *J. Pet. Sci. Eng.* **2015**, *133*, 507–517. [CrossRef]
36. Huang, S.; Cawthorne, C.E. Method for Simulating Drilling of Roller Cone Bits and Its Application to Roller Cone Bit Design and Performance. U.S. Patent 6,516,293 B1, 4 February 2003. Available online: https://patents.google.com/patent/US6516293 (accessed on 10 April 2023).
37. Mazen, A.Z.M. Assessment and Modelling of Wear prediction and Bit Performance for Roller Cone and PDC Bits in Deep Well Drilling. 2020. Available online: https://bradscholars.brad.ac.uk/handle/10454/19171 (accessed on 1 May 2023).
38. Hareland, G.; Wu, A.; Rashidi, B. A Drilling Rate Model for Roller Cone Bits and Its Application. In Proceedings of the International Oil and Gas Conference and Exhibition in China, Beijing, China, 8–10 June 2010; Volume 1, pp. 108–114. [CrossRef]
39. Ju, G.; Yan, T.; Sun, X. Numerical Simulation of Effective Hole Cleaning by Using an Innovative Elliptical Drillpipe in Horizontal Wellbore. *Energies* **2022**, *15*, 399. [CrossRef]

40. Kirencigil, E. Numerical Modeling of the Hydraulics of the Drilling Process Using PDC Drill Bit. 2017. Available online: https://etd.ohiolink.edu/apexprod/rws_etd/send_file/send?accession=akron1514989334702696&disposition=inline (accessed on 1 November 2022).
41. Sivagnanam, M. PDC Drill Bit Redesign and Simulation for Optimized Performance. 2014. Available online: https://prism.ucalgary.ca/bitstream/handle/11023/1709/ucalgary_2014_sivagnanam_mohan.pdf;jsessionid=A35A15E30926CC651D94E9ADAE765528?sequence=2 (accessed on 1 November 2022).
42. Wells, M.R.; Pluere, I.; Pessier, R.C.; Hughes/Christensen. The Effects of Bit Nozzle Geometry on the Performance of Drill Bits. In Proceedings of the AADE National Technical Conference and Exhibition, Houston, TX, USA, 1–3 April 2003; pp. 1–23. Available online: https://www.aade.org/application/files/2715/7304/4602/AADE-03-NTCE-51-Wells.pdf (accessed on 1 May 2023).